Using an iterated block particle filter via **spatPomp**

Ning Ning and Edward L. Ionides

This version compiled on October 25, 2024, using R 4.4.1, **spatPomp** 0.37.0, and **pomp** 5.11.0.1

Source code at `https://github.com/ionides/ibpf-tutorial`

R script at `https://github.com/ionides/ibpf-tutorial/blob/main/ms.R`

Abstract

The IBPF algorithm studied by Ning and Ionides (2023) and Ionides et al. (2024) has been contributed to the R package **spatPomp** (Asfaw et al., 2021, 2024) as the function `ibpf`. This document introduces `ibpf` and validates its correctness on a simple Gaussian example which is tractable using the Kalman filter. We also test `ibpf` on simulated data for a measles transmission model.

Contents

1 A toy example: Correlated Gaussian random walks **2**

2 A measles model **7**

3 Diagnostics **12**

4 Discussion **16**

1 A toy example: Correlated Gaussian random walks

Consider spatial units $1, \dots, U$ located evenly around a circle, where $\text{dist}(u, \tilde{u})$ is the circle distance,

$$\text{dist}(u, \tilde{u}) = \min\big(|u - \tilde{u}|, |u - \tilde{u} + U|, |u - \tilde{u} - U|\big).$$

The latent process is a U-dimensional Brownian motion $\boldsymbol{X}(t)$ having correlation that decays with distance. Specifically,

$$dX_u(t) = \sum_{\tilde{u}=1}^{U} \rho_u^{\text{dist}(u,\tilde{u})}\, dW_{\tilde{u}}(t),$$

where $W_1(t), \dots, W_U(t)$ are independent Brownian motions with infinitesimal variance σ_u^2, and $|\rho_u| < 1$. An observation Y_n is made at each time $t_n = n$ for $n = 1, 2, \dots, N$, and we write $X_n = X(t_n)$. We suppose our measurement model for discrete-time observations of the latent process is

$$Y_{u,n} = X_{u,n} + \eta_{u,n}$$

where $\eta_{u,n} \overset{\text{iid}}{\sim} \text{Normal}(0, \tau_u^2)$. The model is completed by providing the initial conditions, $\{X_u(0), u \in 1 : U\}$, at time $t_0 = 0$. These initial conditions are specified as parameters. An instance of this model is generated below, using the `bm2` function.

```
library(spatPomp)
i <- 2
U <- 4
b <- bm2(U=U,N=switch(i,10,200),unit_specific_names="rho")
plot(b)
```

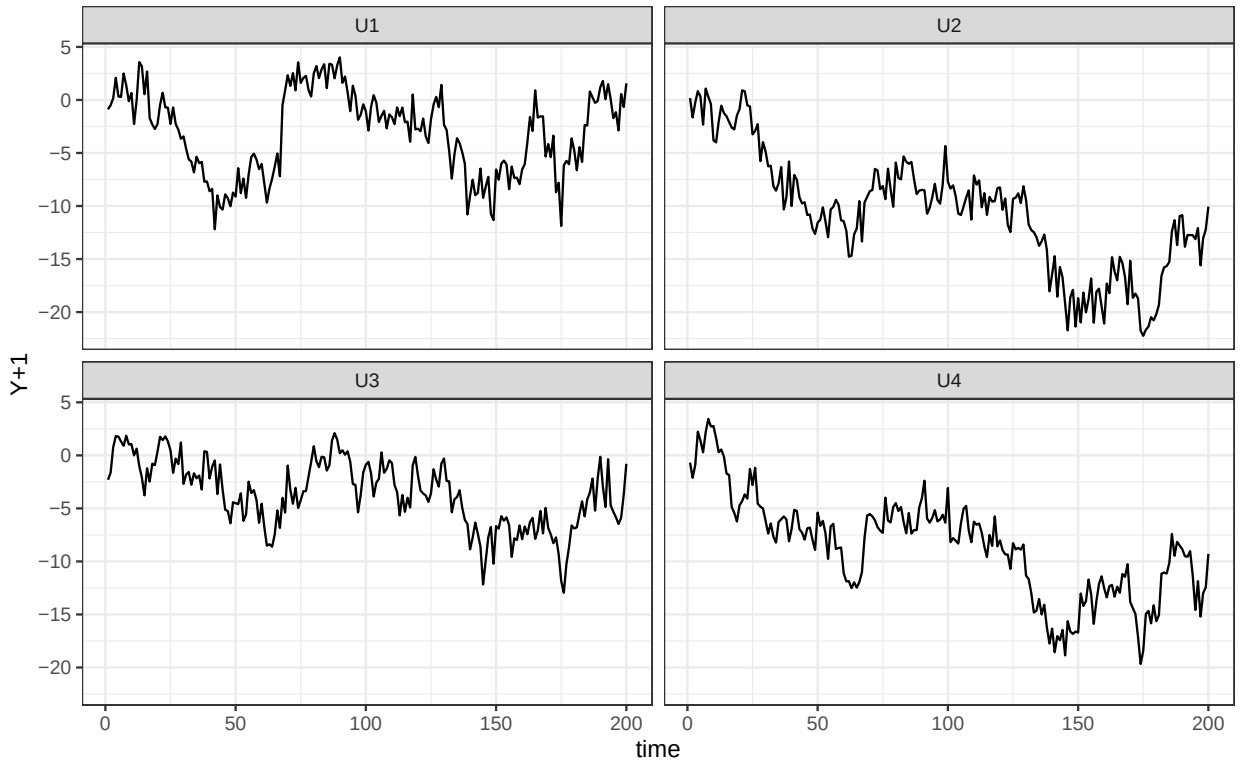

		KF	PF	BPF ($K = 1$)	BPF ($K = 2$)	BPF ($K = 4$)
Log-likelihood	mean	-1472.69	-1480.79	-1477.88	-1509.06	-1547.80
	sd	0.00	3.96	4.00	2.07	1.49

Table 1: Likelihood evaluation for the `bm2` model object, `b`, using the Kalman filter (KF), particle filter (PF), and block particle filter (BPF) with varying numbers of blocks (K). For Monte Carlo filters, the mean and standard deviation are shown for 10 replicates.

Here, `i` is a computational intensity switch which adjusts the code for varying run-time. We set `i=1` for testing and debugging, and `i=2` for higher quality results. For simplicity, we consider only one unit-specific parameter, ρ_u, with other parameters being fixed at a value shared between units. The simulation for `b` has $\rho_u = 0.4$ for all u, but the estimators do not know this. Before carrying out inference, we check likelihood evaluation. For this toy model, the **spatPomp** function `bm2_kalman_logLik` provides an exact log-likelihood via the Kalman filter. This study uses a small number of units ($U = 4$) so that the particle filter is numerically tractable. We use the particle filter provided by the **pomp** package (King et al., 2016), taking advantage of the class structure where class '`spatPomp`' inherits from class '`pomp`'. We can readily validate the agreement between `bm2_kalman_logLik` and `pfilter`, and identify the likelihood cost of the block filter approximation in this situation.

```
kf_logLik <- bm2_kalman_logLik(b)
pf_logLik <- replicate(10,
  logLik(pfilter(b,switch(i,10,1000)))
)
bpf_logLik2 <- replicate(10,
  logLik(bpfilter(b,switch(i,10,1000),block_size=2))
)
```

Table 1 shows the increasingly negative bias, and decreasing variance, of BPF as the number of blocks increases. For a single block, $K = 1$, the BPF algorithm matches PF. PF provides an unbiased estimate of the likelihood, and due to the convexity of the logarithm it has negative bias (approximately equal to half the variance) for estimating the log-likelihood. Subsequently, we investigate inference for $\rho_{1:4}$ with $K = 2$.

Ionides et al. (2023) investigated a range of values for U for this model in their Figure 1, and for an epidemiological model their Figure 3. The small scenario considered here, with $U = 4$, is designed for the following purposes: (i) to validate whether or not `ibpf` is correctly coded by comparison with direct calculations using the Kalman filter; (ii) to check whether or not the block approximation has considerable adverse effects on inference in this case. The inherent scalability of BPF and IBPF, together with the spatial homogeneity of the model, suggests that results for $U = 4$ should be representative for larger U.

For our test of IBPF, we start searches at $\rho_u = u/5$ to investigate the effect (if any) on starting value.

```
rho_start <- seq(from=0.2,to=0.8,length.out=U)
params_start <- coef(b)
params_start[paste0("rho",1:U)] <- rho_start
ibpf_mle_searches <- foreach(reps=1:switch(i,3,10))%dopar%{
  ibpf(b,params=params_start,
    Nbpf=switch(i,2,50),Np=switch(i,10,1000),
    rw.sd=rw_sd(rho1=0.02,rho2=0.02,rho3=0.02,rho4=0.02),
    unitParNames="rho",
    sharedParNames=NULL,
    block_size=2,
    cooling.fraction.50=0.5
  )
}
```

To assess the success of these searches, we evaluate the likelihood of the resulting parameter estimates using the Kalman filter. The highest likelihood found in these ten searches was -1472.27 which is not far from the actual maximum of -1472.11. However, the median of -1474.34 reveals that substantial Monte Carlo maximization error is present. On harder problems, it can be intractable to increase computational effort to the point where the Monte Carlo error is negligible, and instead we emphasize methods that quantify and control the error.

The MLE may be of less interest than marginal confidence intervals for each unit-specific parameter. Therefore, we compute a profile likelihood for ρ_u, using Monte Carlo adjusted profile methodology (Ionides et al., 2017; Ning et al., 2021). We compare this with an exact likelihood profile constructed by numerical optimization of the log-likelihood evaluated using the Kalman filter. The IBPF implementation is identical to the search above, except that the profiled parameter is fixed. For the profile shown in Figure 1, we first evaluate the likelihood using BPF rather than the Kalman filter, to present methodology applicable to non-Gaussian models. We then check against the likelihood evaluated via the Kalman filter for the IBPF estimates, and the profile computed directly from the Kalman filter. These reveal a distinct bias in the IBPF/BPF profile, apparently primarily to do with a bias in likelihood evaluation. The parameter in question describes a dynamic coupling between the units, and a heuristic explanation may be that the blocking procedure breaks some of the coupling and thereby leads to a higher inferred value of the coupling parameter to counterbalance that bias. The bottom panel of Figure shows that we can also diagnose this effect using the particle filter, on this small example for which the particle filter is tractable.

The profile maximization took 18.60 mins using 36 computing cores.

We now do the same calculation for σ, shown in Figure 2, for comparison with ρ. There is some evidence of a bias for σ, but the issue appears to be more severe for ρ.

In Figures 2 and 1, we see that the particle filter provides a close approximation to the exact likelihood, though even for 4 units the variablility is noticeable. Comparison with PF for a small number of units can be used to assess BPF and IBPF for a metapopulation model. We will see below that this model is well suited to BPF and IBPF. Intuitively, this may be because the coupling between units is weak—population movement between towns is critical to disease dynamics, but the vast majority of transmission occurs among residents of the same town.

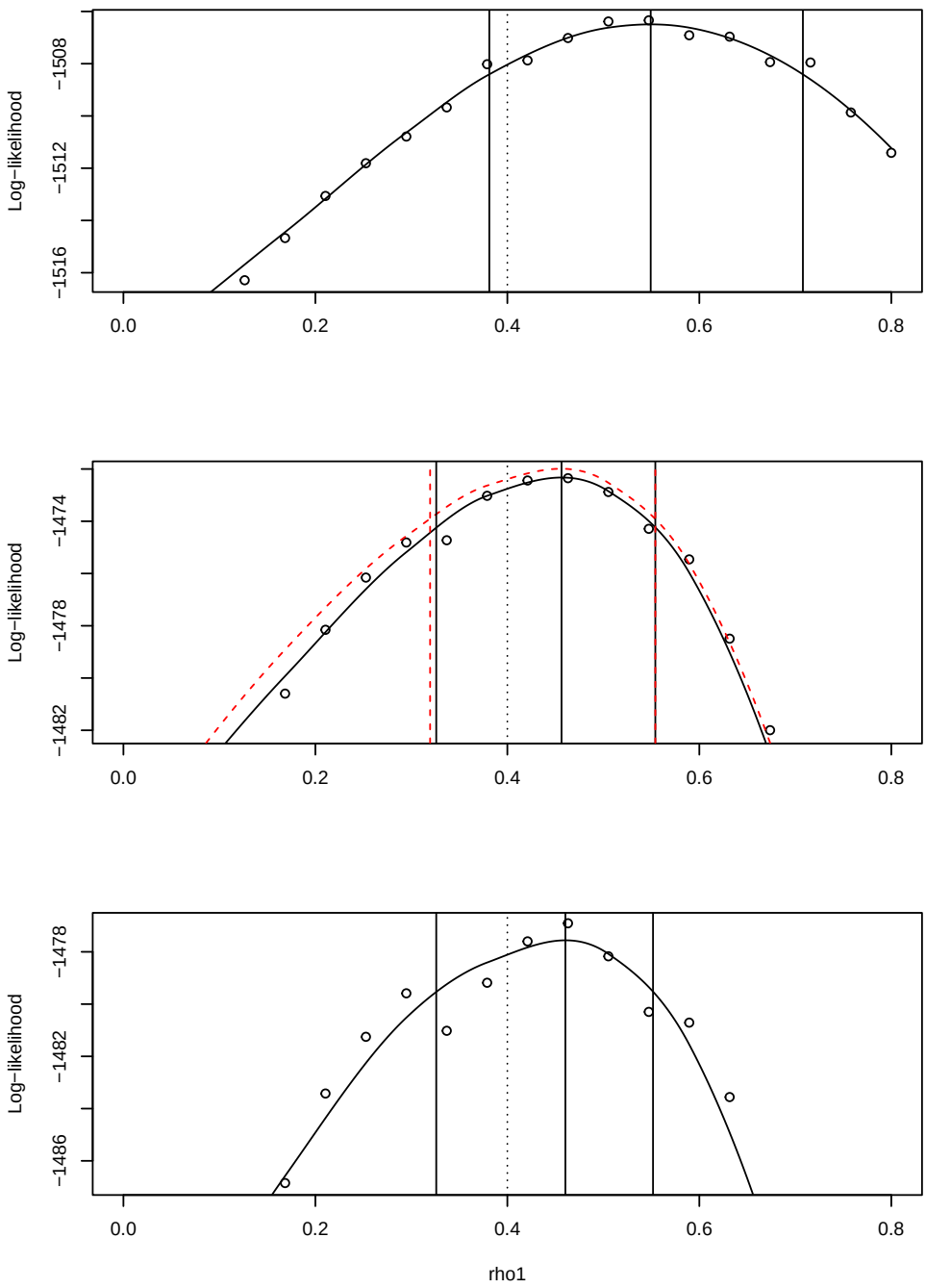

Figure 1: Top: profile for ρ_1 using an IBPF search with likelihood computed using BPF, for $K = 2$ blocks each having 2 units. Middle: Exact profile (dashed red line) and the same IBPF search with likelihood computed exactly using the Kalman filter. Bottom: The same IBPF search with likelihood computed using the particle filter. Vertical lines show the MLE and a 95% confidence interval, with a dotted line at the true parameter value.

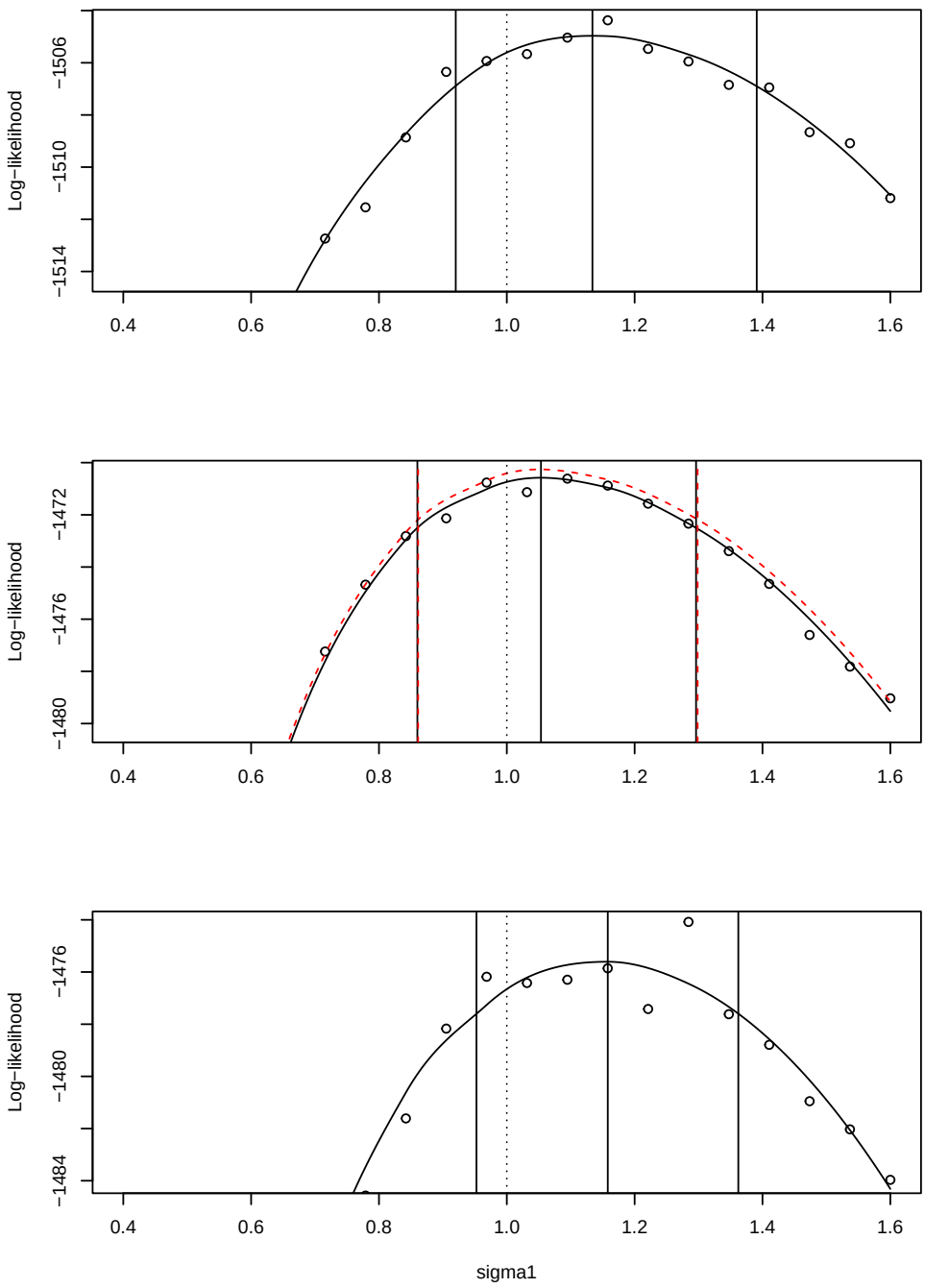

Figure 2: Top: profile for σ_1 using an IBPF search with likelihood computed using BPF, for $K = 2$ blocks each having 2 units. Middle: Exact profile (dashed red line) and the same IBPF search with likelihood computed exactly using the Kalman filter. Bottom: The same IBPF search with likelihood computed using the particle filter. Vertical lines show the MLE and a 95% confidence interval, with a dotted line at the true parameter value.

		PF	BPF ($K = 1$)	BPF ($K = 2$)	BPF ($K = 4$)
Log-likelihood	mean	-10840.70	-10852.00	-10782.31	-10778.67
	sd	12.26	20.19	2.52	2.35

Table 2: Likelihood evaluation for the `he10` model object, `m`, using the particle filter (PF), and block particle filter (BPF) with varying numbers of blocks (K). The mean and standard deviation are shown for 10 replicates with 10^4 particles.

2 A measles model

We now proceed to carry out a similar analysis for the measles model generated by the **spatPomp** function `he10`. This is a susceptible-exposed-infected-recovered model for measles transmission, described by Ionides et al. (2024) and Asfaw et al. (2024). For this model, exact likelihood evaluation is not available. However, for a relatively small number of units ($U = 4$) the particle filter provides an adequate approximation. Ionides et al. (2024) considered fitting this model to data using IBPF, with 20 cities and up to 20×13 parameters. Here, our task is to focus on a smaller, simulated dataset, estimating fewer parameters in order to assess more clearly whether or not the block approximation is leading to substantial bias. We choose two large towns (London and Birmingham) and two small towns (Cardiff and Hastings) since we expect that population movement from large towns to small towns is essential to explain disase persistence in small towns. Large towns can maintain an ongoing epidemic, but below a critical community size local extinction of the disease is expected during epidemic troughs.

```
he10_model <- he10(U=4,dt=1/365,Tmax=switch(i,1955,1964),
  expandedParNames=c("R0"),
  towns_selected=c(1,2,11,12),
  basic_params = c(
    alpha =0.99,      iota=0,          R0=30,
    cohort=0.5,  amplitude=0.3,     gamma=52,
    sigma=52,           mu=0.02,  sigmaSE=0.05,
    rho=0.5,           psi=0.1,          g=800,
    S_0=0.036,         E_0=0.00007,   I_0=0.00006
  )
)
m <- simulate(he10_model,seed=27)
```

Likelihood evaluation took 3.50 mins. Recall that the bias-variance trade-off for likelihood evaluation becomes a tradeoff between two sources of bias for log-likelihood evaluation, due to Jensen's inquality. Table 2 shows that little likelihood is lost due to the block approximation for small numbers of units. Indeed, even for a large number of particles, a small block size gives higher log-likelihood estimates. This is in contrast to the results in Table 1 for the spatially correlated random walk example in Section 1.

Accurate BPF likelihood evalution for a small number of units suggests that the accuracy will persist for larger numbers of units. It is hard to directly test this for the measles model, since we do not have an alternative accurate evalation once PF becomes inapplicable. However, BPF has

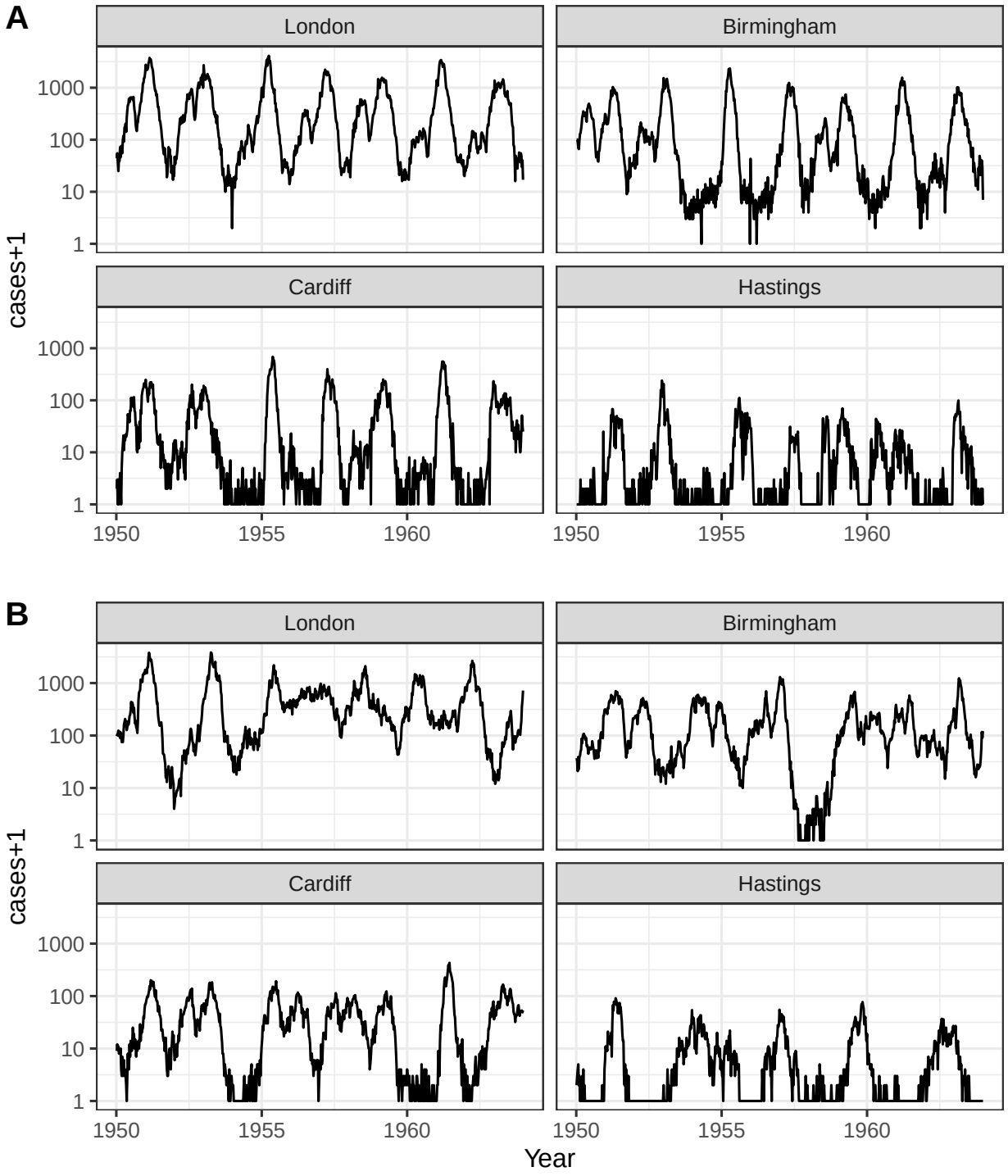

Figure 3: Weekly measles case reports. (A) Data for four UK towns. (B) Simulated data.

favorable scaling properties, and if the weak coupling that makes BPF accurate on the small system is also a feature of the big system, it may be reasonable to expect accuracy in situations where it cannot be directly tested.

The $R0_1$ profile took 337.17 mins using 36 computing cores. Subsequent likelihood evaluation at the proposed profile points took 256.72 mins, for BPF and PF combined. Accurate evaluation of the likelihood is important for inference, and optimization has been empirically found to require fewer particles than evaluation. This is a large computing time for one profile with only 4 units. Perhaps satisfactory results could have been generated more quickly, but generally one expects that simulation based inference for highly nonlinear and non-Gaussian spatiotemporal systems is going to require a considerable amount of computation.

If IBPF is effectively maximizing the BPF approximation to the likelihood, then situations where BPF has low likelihood evaluation bias may correspond to situations where IBPF has low estimation bias. A profile likelihood for one parameter is presented to support this, in Figure 4. Here, the evaluation using PF gives a slightly tighter estimate of the profile, but this may be less accurate: PF is a higher variance algorithm, even with $U = 4$, and its variance increases as the model becomes increasingly misspecified. Thus, the profile likelihood estimate may have additional curvature due to increasing variance (and therefore increasing Jensen bias) away from the MLE.

The block approximation in BPF concerns dependence between blocks and therefore may have an effect on estimation of parameters describing the coupling between units. The measles metapopulation model has a so-called gravity model for coupling, with a parameter g_u controlling the rate of transmission from other cities into city u. A relatively straightforward way to investigate estimation of g_u using BPF and IBPF is to compute a likelihood slice through the true parameter value for a simulation, with only g_u being varied. Here, we investigate a slice for $u = 4$. A likelihood profile cannot take a lower value than a likelihood slice, since the profile has an additional optimization. Therefore, a flat slice implies a flat profile; the converse is not necessarily true. Clear evidence of bias in a slice for a small number of units would anticipate difficulties when undertaking the more time-consuming task of obtaining a profile with many units and many parameters. Figure 5 is consistent with a small positive bias: BPF ignores part of the dependence in the filter distribution, so it may be expected that it compensates by a bias toward parameter values that increase the coupling.

A slice is equivalent to a profile with only a single estimated parameter, so we can construct a Monte Carlo adjusted profile confidence interval under this assumption. The g_4 slice took 15.40 mins using 36 computing cores, which was considerably less computational effort than was used for the profile. Typically, sliced likelihood plots are a computationally convenient tool used for preliminary investigations, and a full profile is preferred for a final conclusion.

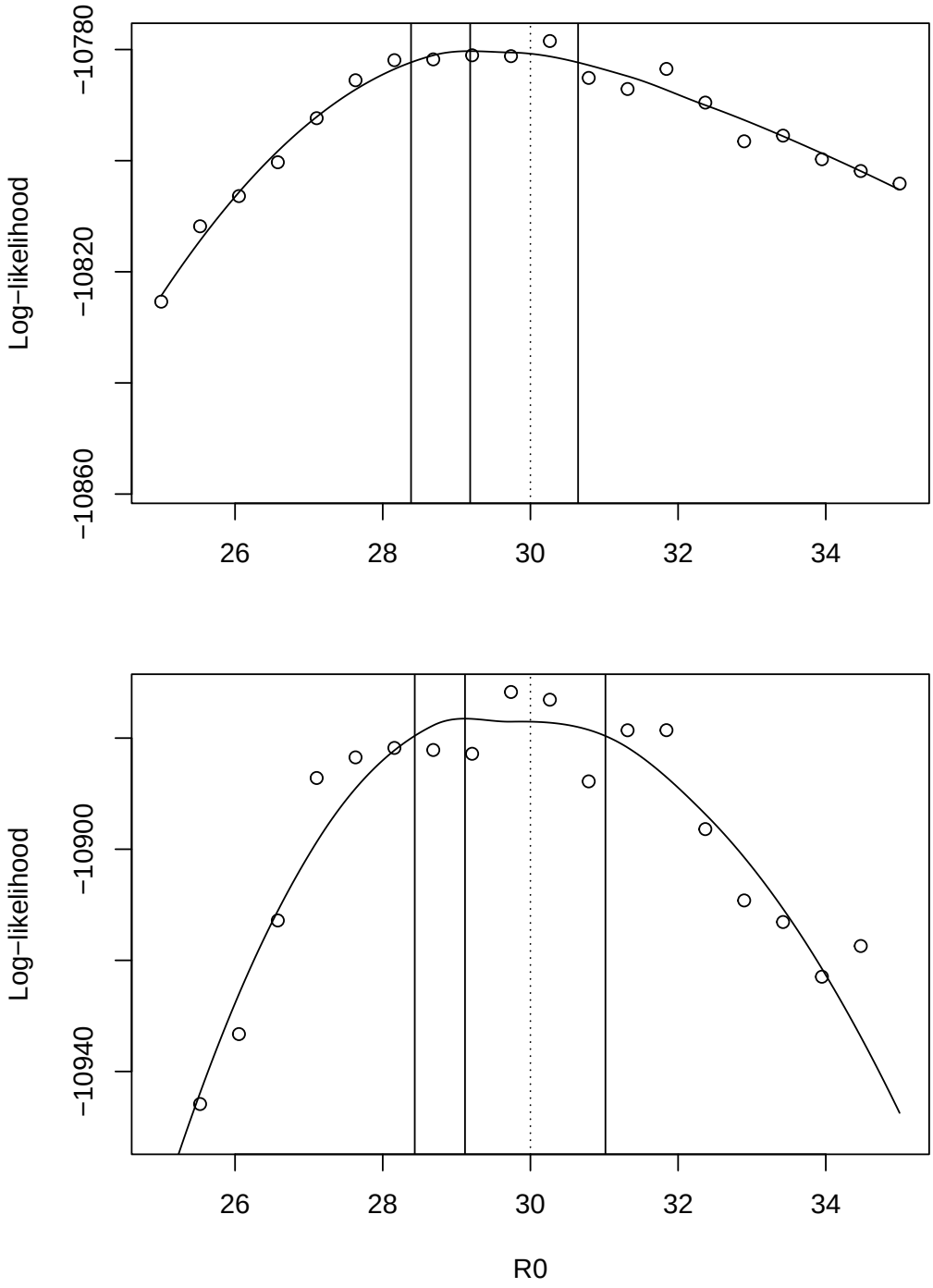

Figure 4: Top: profile for $R0_1$ using an IBPF search with likelihood computed using BPF, for $K = 4$ blocks each having 1 unit. Bottom: The same IBPF search with likelihood computed using the particle filter. Vertical lines show the MLE and a 95% confidence interval, with a dotted line at the true parameter value.

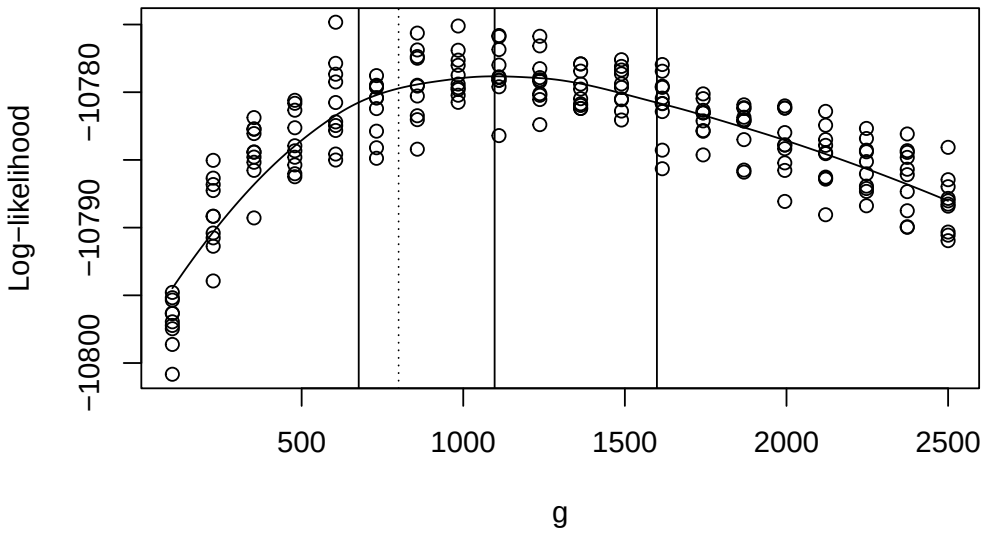

Figure 5: Slice for g_4 through the true parameter vector, using BPF evaluation with $K = 4$ blocks each having 1 unit. Vertical lines show the MLE and a 95% confidence interval, with a dotted line at the true parameter value.

3 Diagnostics

If likelihood maximization appears to be failing, or has unacceptably high Monte Carlo variability, one wishes to diagnose the cause, or causes. Even if inference appears to be operating satisfactorily, it is good practice to see whether there are some data points for which the model is inappropriate, or some parameters for which optimization is less stable. It may be interesting to know if less Monte Carlo effort would be sufficient, or if greater effort would be beneficial. For all these questions, a starting point is exploratory analysis of diagnostic data produced by `ibpf` and `bpfilter`.

The success of an iterated filter for likelihood maximization depends on the success of a single pass of that filter for likelihood evaluation. A useful diagnostic quantity for the particle filter is the effective sample size (ESS) (Doucet and Johansen, 2011; Liu, 2001). In the notation of King et al. (2016), the filter observation weight for particle j at time n is $w(n,j) = f_{Y_n|X_n}(y_n^*|X_{n,j}^P;\theta)$, the normal weight is $\tilde{w}(n,j) = w(n,j)\big/\sum_{k=1}^J w(n,k)$, and the effective sample size is

$$\mathrm{ESS}_n = \left(\sum_{j=1}^J \tilde{w}(n,j)^2\right)^{-1}. \tag{1}$$

ESS is generally motivated as an approximation to the equivalent number of independent samples from the filtering distribution. In the context of likelihood-based inference, it is convenient to think of ESS_n^{-1} as an approximation to the variance of the conditional log-likelihood estimate,

$$\hat{\ell}_n = \log\left(\frac{1}{J}\sum_{j=1}^J w(n,j)\right). \tag{2}$$

However, ubiquitous multi-core computation permits us to calculate this variance directly, by Monte Carlo replication. This bypasses consideration of whether or not ESS is a good estimator. Also, the Monte Carlo replicates, denoted by $\hat{\ell}_n^{(r)}$, for $r = 1,\dots,R$, give rise to an improved estimate of the conditional log-likelihood,

$$\bar{\ell}_n = \frac{1}{R}\sum_{r=1}^R \hat{\ell}_n^{(r)}, \tag{3}$$

together with an uncertainty estimate via the central limit theorem. One could also replace the arithmetic average in (3) using `pomp::logmeanexp`.

Figure 6 shows both ESS and conditional log-likelihood variance (CLLV) for measles in London. We see that both measures agree on the most problematic observations. However, ESS is not a sensitive proxy for CLLV elsewhere in the distribution. CLLV can be calculated for each observation time (cumulative over all units) for a block particle filter, but for diagnostic purposes we write the conditional log-likelihood as a sum of block conditional log-likelihood (BCLL) values. Using the notation of Asfaw et al. (2024), the weights for block $\mathcal{B}_k \subset 1{:}U$ are

$$w_{k,n}^j = \prod_{u\in\mathcal{B}_k} f_{Y_{n,n}|X_{u,n}}\big(y_{u,n}^* \,|\, X_{u,n}^{P,j};\theta\big). \tag{4}$$

The BCLL is

$$\hat{\ell}_{k,n} = \frac{1}{J}\sum_{j=1}^J w_{k,n}^j, \tag{5}$$

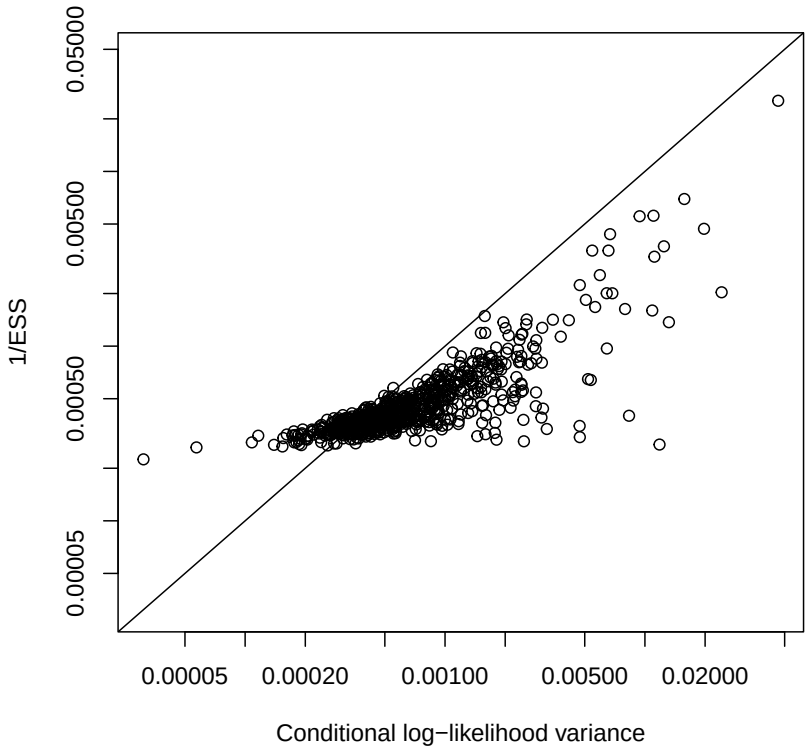

Figure 6: Comparison of effective sample size and conditional log-likelihood variance for measles in London

and the block approximation to the conditional likelihood of $y_1^*, \ldots, y_U^*$ is

$$\hat{\ell}_n = \sum_{k=1}^{K} \hat{\ell}_{k,n}. \tag{6}$$

For our measles spatPomp example, we calculate the BCLL and its variance (BCLLV) as follows:

```
bpf_list <- foreach(rep=1:switch(i,6,40)) %dopar% {
  bpfilter(he10_model,Np=switch(i,10,2000),block_size=1)
}
bpf_ll  <- sapply(bpf_list,function(x)x@block.cond.loglik)
dim(bpf_ll) <- c(dim(bpf_list[[1]]@block.cond.loglik),length(bpf_list))
bcll <- apply(bpf_ll,c(1,2),mean)
bcllv <- apply(bpf_ll,c(1,2),var)
```

Once we have identified that an observation is hard to filter, there are various classes of explanation: (i) the data point is an outlier, which any reasonable model would struggle to explain; (ii) the model is poor at that point; (iii) there is no problem with the model or data, but the system happens to require a high Monte Carlo effort at that point. Neither ESS nor CLLV can distinguish these alternatives. It can be helpful to compare the model fit against a simple statistical model, to provide an objective benchmark. Measles case counts are an example of a population system exhibiting exponential growth and decay, and in such cases a log-scale autoregressive moving average (log-ARMA) model can provide an appropriate benchmark. The function `spatPomp::arma_benchmark` fits this model for each unit of a `spatPomp` object and provides the unit conditional log-likelihood values for each time point. Here, blocks are taken to be units, so we define the log-likelihood anomaly as the difference between the BCCL and the unit benchmark,

```
benchmark <- arma_benchmark(he10_model)
anomaly <- bcll - benchmark$cond
```

Unlike BCLL, both log-likelihood anomaly and BCLLV have the convenient property that they do not depend on the scale of the data, or the units in which it is measured.

Figure 7 investigates two units—London and Birmingham—via BCLLV and log-likelihood anomaly. We see that the model used here fits London well and Birmingham poorly. Some time points have very high Monte Carlo likelihood estimate variance, and those points also have poor likelihood compared to the benchmark. One observation for London has a poor log-likelihood anomaly but a decent BCLLV. For Birmingham, both anomaly and BCLLV lead the same conclusion that the model is unsatisfactory, at these default initial parameter values. Here, our goal is only to check methods on simulated data, but if we wanted to fit the model to data, we should confirm whether the diagnostics from the final fitted model have improved.

Log-likelihood anomalies can be plotted against any covariate of interest for exploratory data analysis. This is analogous to residual analysis for linear models.

Trace plots to check on the convergence of `ibpf` are similar to those for other iterated filtering algorithms. In Figure 8, we show this for the Gaussian correlated random walk example. In this case, we see replicable convergence among independent searches. The likelihood rises toward the

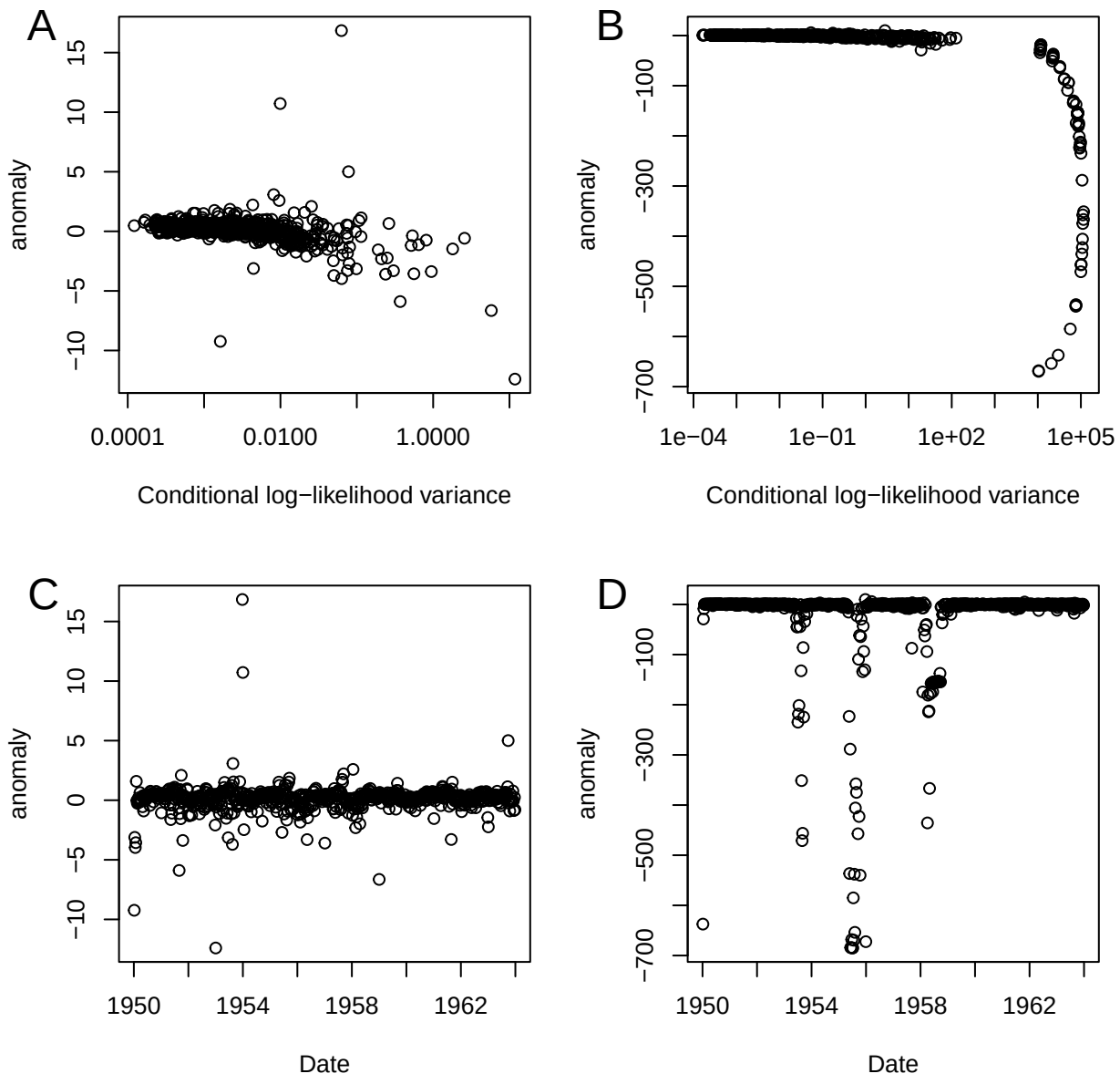

Figure 7: Block particle filter diagnostics for London (A,C) and Birmingham (B,D).

maximum and then stabilizes in a neighborhood of the maximum while the estimated parameters explore this region.

```
ibpf_traces <- pomp::melt(lapply(ibpf_mle_searches,pomp:::traces_internal))
ibpf_traces$iteration <- as.numeric(ibpf_traces$iteration)
ggplot(ibpf_traces, aes(x=iteration,y=value,group=.L1,color=factor(.L1))) +
  geom_line() +
  guides(color="none") +
  facet_wrap(~variable,scales="free_y")
```

4 Discussion

Further examples of `ibpf` being used for data analysis are provided by Li et al. (2024) and Wheeler et al. (2024). Li et al. (2024) studied the spread of COVID-19 in China at the start of the pandemic. Their models are available in the `metapoppkg` R package (`https://doi.org/10.5281/zenodo.10149233`) and the article source code is available at `https://doi.org/10.5281/zenodo.10149258`. Wheeler et al. (2024) studied a cholera epidemic in Haiti. Their models are available in the `haitipkg` R package (`https://doi.org/10.5281/zenodo.7557099`) and the article source code is available at `https://doi.org/10.5281/zenodo.10783080`.

Acknowledgments

We are grateful to Ben Bolker for providing useful feedback.

References

Asfaw, K., Ionides, E. L., and King, A. A. (2021). `spatPomp`: R package for statistical inference for spatiotemporal partially observed Markov processes. `https://cran.r-project.org/web/packages/spatPomp`.

Asfaw, K., Park, J., King, A. A., and Ionides, E. L. (2024). A tutorial on spatiotemporal partially observed Markov processes via the R package spatpomp. *arXiv:2101.01157v4*.

Doucet, A. and Johansen, A. (2011). A tutorial on particle filtering and smoothing: Fifteen years later. In Crisan, D. and Rozovsky, B., editors, *Oxford Handbook of Nonlinear Filtering*, pages 656–704. Oxford University Press.

Ionides, E. L., Asfaw, K., Park, J., and King, A. A. (2023). Bagged filters for partially observed interacting systems. *Journal of the American Statistical Association*, 118:1078–1089.

Ionides, E. L., Breto, C., Park, J., Smith, R. A., and King, A. A. (2017). Monte Carlo profile confidence intervals for dynamic systems. *Journal of the Royal Society Interface*, 14:1–10.

Ionides, E. L., Ning, N., and Wheeler, J. (2024). An iterated block particle filter for inference on coupled dynamic systems with shared and unit-specific parameters. *Statistica Sinica*, 34:1145–1166.

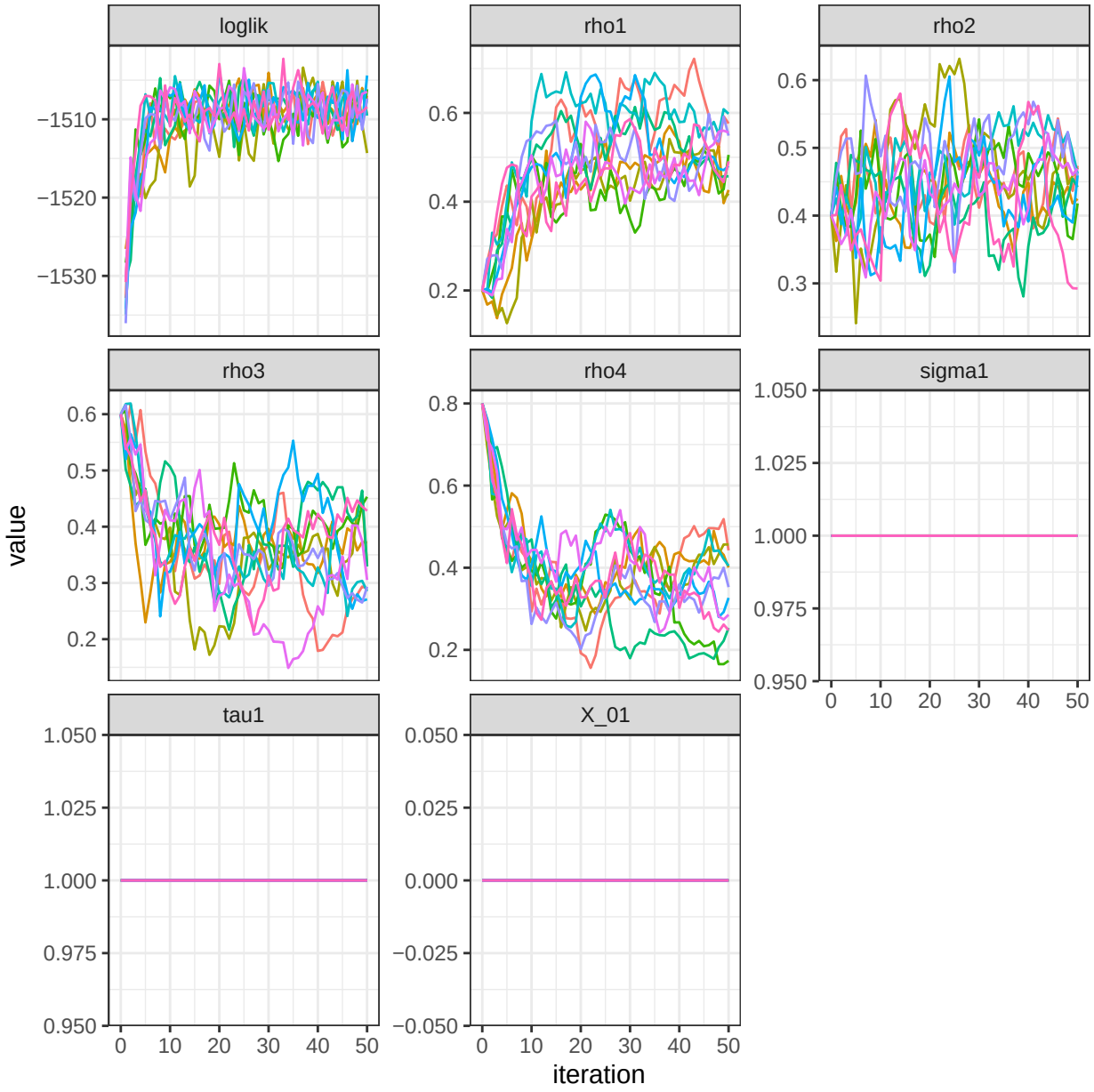

Figure 8: Trace plots for the correlated Gaussian random walk example. Constant traces for σ_1, τ_1 and $X_{0,1}$ arise because these parameters are treated as known and not estimated. Note that the values of σ_1, τ_1 and $X_{0,1}$ are shared across units (e.g., there is no σ_2) since the `bm2` constructor is called with ρ as the only unit-specific parameter.

King, A. A., Nguyen, D., and Ionides, E. L. (2016). Statistical inference for partially observed Markov processes via the R package pomp. *Journal of Statistical Software*, 69:1–43.

Li, J., Ionides, E. L., King, A. A., Pascual, M., and Ning, N. (2024). Inference on spatiotemporal dynamics for networks of biological populations. *Journal of the Royal Society Interface*, 21:20240217.

Liu, J. S. (2001). *Monte Carlo Strategies in Scientific Computing*. Springer, New York.

Ning, N. and Ionides, E. L. (2023). Iterated block particle filter for high-dimensional parameter learning: Beating the curse of dimensionality. *Journal of Machine Learning Research*, 24(82):1–76.

Ning, N., Ionides, E. L., and Ritov, Y. (2021). Scalable Monte Carlo inference and rescaled local asymptotic normality. *Bernoulli*, 27:2532–2555.

Wheeler, J., Rosengart, A., Jiang, Z., Tan, K., Treutle, N., and Ionides, E. L. (2024). Informing policy via dynamic models: Cholera in Haiti. *PLOS Computational Biology*, 20:e1012032.